



pHEMA@AGMNA-1: A novel material for the development of antibacterial contact lens

A.K. Rossos^a, C.N. Banti^{a,*}, A.G. Kalampounias^b, C. Papachristodoulou^c, K. Kordatos^d, P. Zoumpoulakis^e, T. Mavromoustakos^f, N. Kourkoumelis^g, S.K. Hadjidakou^{a,h,**}

^a Section of Inorganic and Analytical Chemistry, Department of Chemistry, University of Ioannina, Greece

^b Physical Chemistry Laboratory, Department of Chemistry, University of Ioannina, Greece

^c Department of Physics, University of Ioannina, Greece

^d Laboratory of Inorganic and Analytical Chemistry, School of Chemical Engineering, National Technical University of Athens, Greece

^e Institute of Biology, Medicinal Chemistry and Biotechnology, National Hellenic Research Foundation, Athens, Greece

^f Organic Chemistry Laboratory, Department of Chemistry, National and Kapodistrian University of Athens Greece, Greece

^g Medical Physics Laboratory, Medical School, University of Ioannina, Greece

^h University Research Center of Ioannina (URCI), Institute of Materials Science and Computing, Ioannina, Greece

ARTICLE INFO

Keywords:

Antimicrobial materials

Hydrogels

Antibacterial active contact lens

Microbial keratitis

ABSTRACT

The Metal Organic Framework (MOF) of formula $\{[Ag_6(\mu_3\text{-HMNA})_4(\mu_3\text{-MNA})_2]^{2-} \cdot [(Et_3NH)^+]_2 \cdot (DMSO)_2 \cdot (H_2O)\}$ (AGMNA), a known efficient antimicrobial compound which contains the anti-metabolite, 2-thio-nicotinic acid (H_2MNA), was incorporated in polymer hydrogels using, hydroxyethyl-methacrylate (HEMA). The material pHEMA@AGMNA-1 was characterized by X-ray fluorescence (XRF) spectroscopy, X-ray powder diffraction analysis (XRPD), Scanning Electron Microscopy (SEM), Energy-dispersive X-ray spectroscopy (EDX), Thermogravimetric Differential Thermal Analysis (TG-DTA), Differential Scanning Calorimetry (DTG/DSC), attenuated total reflection spectroscopy (FT-IR-ATR) and Ultrasonic Imaging. The antimicrobial capacity of pHEMA@AGMNA-1 was evaluated against the Gram negative bacterial strain *Pseudomonas aeruginosa* and the Gram positive ones of the genus *Staphylococcus epidermidis* and *Staphylococcus aureus*, which are the etiology of the microbial keratitis. The % bacterial viability of *P. aeruginosa*, *S. epidermidis* and *S. aureus* upon their incubation with pHEMA@AGMNA-1 discs is significantly low ($0.4 \pm 0.1\%$, $1.5 \pm 0.4\%$ and $7.7 \pm 0.5\%$ respectively). The inhibition zones (IZ) caused by pHEMA@AGMNA-1 discs against *P. aeruginosa*, *S. epidermidis* and *S. aureus* are 14.0 ± 1.1 , 11.3 ± 1.3 and 11.8 ± 1.8 mm respectively. Furthermore, pHEMA@AGMNA-1 exhibits low toxicity. Thus, pHEMA@AGMNA-1 might be an efficient candidate for the development of antimicrobial active contact lenses.

1. Introduction

Contact lenses are risk factors for developing ocular complications such as microbial keratitis (MK) [1–3]. Although, the incidence of MK is rather low, as compared to other health conditions [4], however, due to the high number of contact lens wearers (45 million in the United States [5]), there are thousands of cases of MK each year. Infections occur due to microbial contamination of contact lenses, lens cases and lens care solution [6,7]. If MK developed it can result in severe visual consequences, sometimes even resulting in corneal perforation [3]. Bacteria such as *Pseudomonas aeruginosa*, *Staphylococcus epidermidis* and *Staphylococcus aureus*, can adhere and colonize to lens materials due to

their ability to grow as a resistant biofilm on lenses [2,6]. Therefore, the use of contact lens, which are made by long term or permanent, antimicrobial materials is a research, technological and financial issue of great importance [7].

One strategy that may help reduce the incidence of bacterial infections is through use of silver(I) complexes due to their remarkable antimicrobial properties [8,9]. Moreover, the increasing microbial resistance against current antibiotics has been reignited the research on silver(I) compounds. Silver nitrate solutions are used for long, as antimicrobial for eye drops [9]. Recently, it was shown that, the combination of silver(I) with ciprofloxacin (a second generation antibiotic of the series of quinolones) forms the bactericidal inorganic–organic

* Corresponding author.

** Correspondence to: S.K. Hadjidakou, Section of Inorganic and Analytical Chemistry, Department of Chemistry, University of Ioannina, Greece.

E-mail addresses: cbanti@uoi.gr (C.N. Banti), shadjika@uoi.gr (S.K. Hadjidakou).

hybrid **CipAg** which exhibits 2–3 folds stronger activity than the commercially available hydrochloride salt of ciprofloxacin [8]. The antimicrobial properties of silver-containing compounds are due either to (i) their interactions with the bacterial cell wall (ii) their interactions with DNA, enzymes, and membrane protein or (iii) they generate Reactive Oxygen Species (ROS) [9].

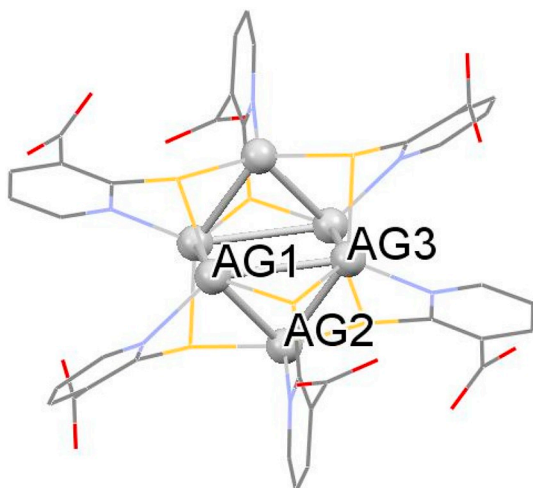
Polymeric hydrogels, which are based on hydroxy ethyl methacrylate (HEMA), are hydrophilic biocompatible materials permeable to water and oxygen making them excellent ingredients for contact lenses formation [10,11]. Moreover, the encapsulation of antimicrobial agents into hydrogels, diffuse their property to the polymeric network itself [8,12]. Silver nanoparticles (Ag-NPs) loaded hydrogels, on the other hand, have been already used for designing antimicrobial coating on contact lenses. Soaked hydrogels with Ag-NPs (10 and 20 ppm) show high activity against *P. aeruginosa* and *S. epidermidis* and they also inhibit the formation of biofilm produced by *S. epidermidis*. Additionally, zinc-doped CuO nanoparticles impart antibacterial properties to the contact lenses [7,13–15].

In the course of our studies on the development of new antimicrobial contact lens [8,16–20] the Metal Organic Framework (MOF) of formula $\{[Ag_6(\mu_3-HMNA)_4(\mu_3-MNA)_2]^{2-} \cdot [(Et_3NH)^+]_2(DMSO)_2(H_2O)\}$ (**AGMNA**) (Scheme 1), was incorporated in polymer hydrogel using, *p*-hydroxyethyl-methacrylate (pHEMA). The material pHEMA@AGMNA-1 was characterized using of multiple techniques including XRF, XRPD, SEM-EDX, TG-DTA, DTG/DSC, FT-IR-ATR and Ultrasonic Imaging. The antimicrobial activity of pHEMA@AGMNA-1 was tested against the bacterial strains *P. aeruginosa*, *S. epidermidis* and *S. aureus*. The *in vivo* toxicity of pHEMA@AGMNA-1 was examined against *Artemia salina* assay.

2. Results and discussion

2.1. General aspects

pHEMA cross-linked with ethylene glycol dimethacrylate (EGDMA) is the basis of many types of daily wearing soft contact lenses [21]. In order to evaluate the antimicrobial efficiency of contact lens which contain antimicrobial agents, a solution of AGMNA (1 mM) was dispersed in pHEMA (Scheme 2) during its polymerization procedure towards the pHEMA@AGMNA-1 formation. The dispersion of AGMNA into pHEMA was qualitatively verified by attenuated total reflection spectroscopy (FT-IR-ATR), Differential Scanning Calorimetry (DTG/DSC) and Ultrasonic Imaging. Since the contained of pHEMA@AGMNA-1 in silver, however, was kept limited on purpose to avoid toxic effects, the metal concentration was kept close to the analysis limits of the techniques. Therefore, a variety of analytical



Scheme 1. Molecular diagrams of AGMNA [20].

techniques such as X-ray fluorescence (XRF) spectroscopy, Energy-dispersive X-ray spectroscopy (EDX) and Thermogravimetric Differential Thermal Analysis (TG-DTA) were used for the quantitative determination of the content of pHEMA@AGMNA-1, in silver.

pHEMA and pHEMA@AGMNA-1 discs of 10 mm diameter were cut, cleaned from monomers and stored either in sterilized NaCl 0.9% w/w solution or they dried at 50 °C (Fig. 1).

In order to ascertain diffusion of AGMNA from the pHEMA@AGMNA-1 the UV–Vis spectra of the supernatant, solution in broth and in double distilled water were recorded before and after incubation with the disc. These spectra are identical with the corresponding ones after 24 h suggesting that no any releasing of the AGMNA from the hydrogel in the medium occurred.

2.2. Refractive index

Since this material is developed for contact lens the refractive index is determined to justify whether the optical property is appropriate for refraction correction. The refractive indexes are quoted in Table 1. Both pHEMA and pHEMA@AGMNA-1 discs stored in water exhibit almost the same refractive indexes (1.437). This value is in accordance to the corresponding one of the pHEMA@platinum-nanoparticles (1.424–1.436) [7].

2.3. X-ray fluorescence spectroscopy

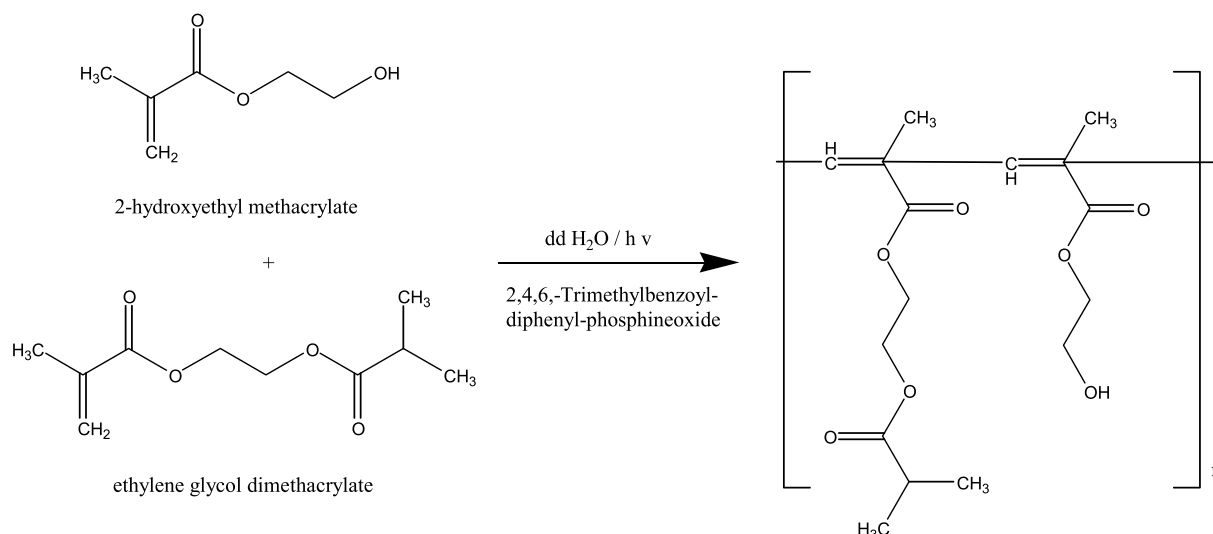
Dry pHEMA@AGMNA-1 discs were grind to powder. The XRF spectrum of pHEMA@AGMNA-1 powder confirms the presence of Ag in the hydrogel which is indicative of the encapsulated AGMNA into the pHEMA (Fig. 2). The content of silver in the hydrogel (pHEMA@AGMNA-1) was determined at $0.19 \pm 0.05\%$ w/w. Therefore a concentration of 2.93 μmol AGMNA/g of hydrogel is found. The calculated, content in the case that all the amount of AGMNA used for the preparation has been incorporated into the material, is 2.95 μmol /g. For comparison the content of silver in AGMNA was also determined by XRF spectroscopy at $36.4 \pm 4.6\%$ w/w (calc.: 33.25% w/w).

2.4. X-ray powder diffraction analysis (XRPD)

Powder of dry pHEMA@AGMNA-1 disc was used for XRPD spectrum recording. Fig. 3 shows the X-ray diffraction analysis of pHEMA (A), AGMNA (B) and pHEMA@AGMNA-1 (C), respectively. pHEMA shows broad diffractions characteristics of amorphous framework (Fig. 3A). In case of AGMNA, crystalline phase of the cluster is clearly observed with characteristics diffraction patterns (Fig. 3B). After loading of AGMNA over pHEMA, the spectrum remains similar to that of pHEMA (Fig. 3C). The absence of AGMNA peaks shows the effective phase transition from crystalline to amorphous phase during confinement into pHEMA.

2.5. Scanning Electron Microscopy (SEM), Energy-dispersive X-ray spectroscopy (EDX)

The elemental analysis (% wt) of silver in the pHEMA@AGMNA-1 discs was determined by EDX measurements. The content of silver in pHEMA@AGMNA-1 is 0.26651% w/w. This leads to a concentration of 2.70 μmol of AGMNA per gram of hydrogel, which is in accordance to the corresponding one determined by XRF spectroscopy (2.93 μmol of AGMNA per gram of hydrogel). Considering the concentration of the solution used for the preparation of pHEMA@AGMNA-1 (1 mM) the calculated contain of AGMNA in the hydrogel is 2.95 μmol /g. A typical electron microscopy (SEM) image of pHEMA@AGMNA-1 accompanied by qualitative EDX analysis for AGMNA, is shown in Fig. 4.



Scheme 2. Preparation reaction of pHEMA.

2.6. Thermo gravimetric analysis of the pHEMA and the pHEMA@AGMNA-1

2.6.1. Differential Scanning Calorimetry (DSC)

In order to clarify whether AGMNA and pHEMA interact in the solid state to give a mixture or a composite, DSC studies were carried out on the powder of dry pHEMA and pHEMA@AGMNA-1 discs. DSC thermodiagrams of pHEMA and pHEMA@AGMNA-1 are shown in Fig. 5. The sharp endothermic transition which is observed at 328.88 °C in the DSC diagram of pHEMA, is shifted to lower temperature at 310.48 °C for pHEMA@AGMNA-1 suggesting formation of a composite instead of a mixture in this case.

2.6.2. Thermal decomposition of pHEMA and the composite pHEMA@AGMNA

TG/DTA analysis was performed under air on the powder of dry pHEMA and pHEMA@AGMNA-1 discs, while the temperature increased at a rate of 10 °C/min from ambient up to 500 °C (Fig. S1). The thermal decomposition of pHEMA and pHEMA@AGMNA-1 show endothermic evolution of water at r.t.–200 °C (2.76%) and at r.t.–200 °C (5.73%) respectively. This is occurred because of the hygroscopic character of the polymer. The composite pHEMA@AGMNA-1 decomposes with two endothermic and one exothermic step at 210–300, 300–395 and 440–485 °C (Fig. S1) with total mass loss of 86% which are attributed to the polymer degradation into the HEMA monomer and the release of the AGMNA [22]. The pHEMA decomposes with three endothermic steps at 210–315, 315–380 and 410–460 °C with total mass loss of 91.4% (Fig. S1).

2.7. Attenuated total reflection spectroscopy (ATR)

ATR-FTIR spectroscopy provides information about the presence of AGMNA ingredient of pHEMA matrix from moderate up to severe confinement since the penetration depth is estimated to be up to 20 μm (Fig. 6). The spectrum of the solid AGMNA is also shown for comparison reasons. The spectrum of the unloaded pHEMA matrix was recorded as background and subtracted directly from the spectrum of the corresponding pHEMA@AGMNA-1 matrix. Thus, following this procedure, the excess spectra are compared with the corresponding spectra of the free AGMNA.

Almost all the characteristic bands of AGMNA are also appeared in the excess spectra of the pHEMA matrices loaded with the corresponding material (pHEMA@AGMNA-1) confirming the dispersion of the ingredient into the pHEMA matrix. Any difference in the relative

intensities between the two spectra is reasonable considering the fact that the one spectrum corresponds to a material confined in a matrix, while the other spectrum is recorded from the same solid material dispersed in KBr pellet.

In the low-frequency region attributed mainly to bending modes, the frequencies of the corresponding bands almost coincide between the two spectra suggesting the coexistence of AGMNA in pHEMA. This observation is attributed to confinement effect, where the stretching modes are more affected than the corresponding bending modes. This is expected for stretching modes, since the inter-atomic distance is reduced due to geometric restrictions. Thus, the energy of the vibration increases and its frequency is observed in the spectra as blue shifted [23].

2.8. Ultrasonic Imaging

The transmission of the ultrasound results in a dynamic mechanical stress of high-frequency to the material, which can provide an additional insight into the physicochemical processes occurring during the formation of pHEMA@AGMNA-1 sample.

The interaction of the ultrasonic waves with the microscopic structural features of the material under scattering and absorption mechanisms is reflected in the measured ultrasonic velocity and attenuation that are directly linked with the elastic properties of the studied material [24,25].

In an effort to evaluate the incorporation of the AGMNA into the pHEMA matrix, we measured the sound velocities and attenuation coefficients for the unloaded pHEMA matrix as well as the corresponding values for the loaded pHEMA based samples for all loading concentrations. The evaluation of the results, not only in qualitative but also in quantitative basis, is performed by calculating the ratios of the sound velocities and attenuation coefficients with reference to the unloaded pHEMA matrix. The so-obtained velocity and attenuation ratios are presented in Fig. 7. The decrease of the ultrasonic longitudinal velocity and attenuation ratios reflects the changes of the elastic properties and density through the final material induced by the addition of AGMNA in the pHEMA matrix. The final value of the acoustic attenuation was found lower than the initial one indicating that the acoustic impedance alters by addition of AGMNA, which supports the proposed formation of pHEMA@AGMNA-1.

2.9. Antimicrobial activity of pHEMA@AGMNA-1

The antibacterial efficiency of AGMNA was previous studied [20]. The MIC values of AGMNA (MIC values: 25.7 ± 2.4 and 42 ± 0.3 μM



(A)



(B)



(C)

Fig. 1. Discs of pHEMA@AGMNA-1 in 0.9% NaCl (A) and discs in their dried form of pHEMA (B), pHEMA@AGMNA-1 (C).

Table 1

Refractive indices of the lenses measured at 24 °C.

Stored in	Samples	Refractive index
Water	pHEMA	1.437
	pHEMA@AGMNA-1	1.436
Dry	pHEMA	1.472
	pHEMA@AGMNA-1	1.405

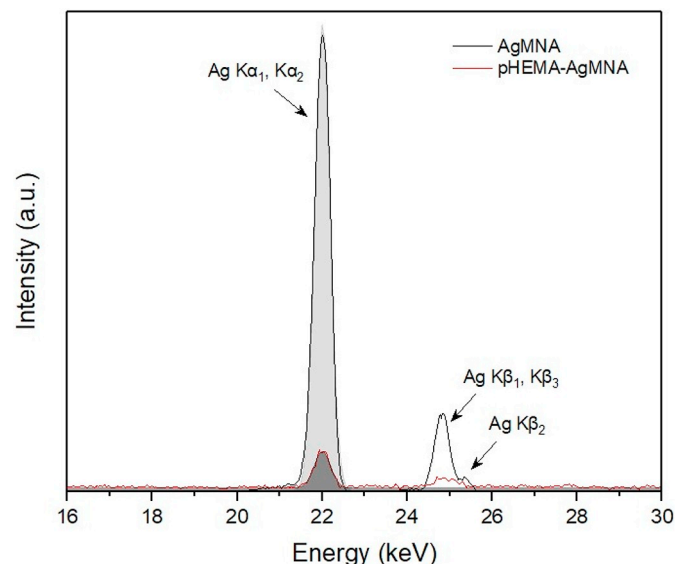


Fig. 2. XRF spectrum of AGMNA and the corresponding one of pHEMA@AGMNA-1. The Ag K α peak was used for quantitative determination of Ag in the samples.

respectively) against *P. aeruginosa* and *S. aureus* are 3-fold stronger than the corresponding ones of silver nitrate, a disinfectant-antiseptic formulation in clinical use (MIC values: 78 ± 1.5 and 126.8 ± 1.0 μM respectively) [20]. The known antimicrobial efficiency of AGMNA led its dispersion in pHEMA in an attempt to investigate the expansion of this property in the hydrogel, as well. In order to evaluate this property, pHEMA@AGMNA-1 and pHEMA discs were placed in test tubes which contain $5 \cdot 10^5$ cfu/mL of *P. aeruginosa*, *S. epidermidis* and *S. aureus* microbes (Fig. 8). The % viability of microbes was calculated by the following equation [18]:

Cell viability(%)

$$= \frac{\text{Optical density of the broth solution at 620 nm}}{\text{Optical density of the control (+) broth solution at 620 nm}} \times 100$$

The calculated bacterial % viability of *P. aeruginosa*, *S. epidermidis* and *S. aureus* upon their incubation with pHEMA@AGMNA-1 discs for 20 h is $0.4 \pm 0.1\%$, $1.5 \pm 0.4\%$ and $7.7 \pm 0.5\%$ respectively as shown in Fig. 8. On the contrary, no influence against these bacterial strains was observed upon their treatment by discs of pure pHEMA (Fig. 8). However, 4 μL of the supernatant of the above solutions colonized agar growth media of plates, indicating that pHEMA@AGMNA-1 discs prevent microbial growth only under their presence (Fig. S2).

The removal of preformed biofilm, caused by pHEMA@AGMNA-1 was also assessed using crystal violet assay [26]: The discs of pHEMA@AGMNA-1, remove preformed biofilm by 28.7% (*P. aeruginosa*) and 39.6% (*S. aureus*) (Fig. S3).

In order to test the sensitivity of bacteria against pHEMA@AGMNA-1 discs, agar diffusion test was developed. In this assay, discs with or without the antimicrobial agents are placed on agar plate which contains the bacterial strains (10^8 cfu/mL). After incubation of bacteria with the tested material, a visible area without bacterial lawn around

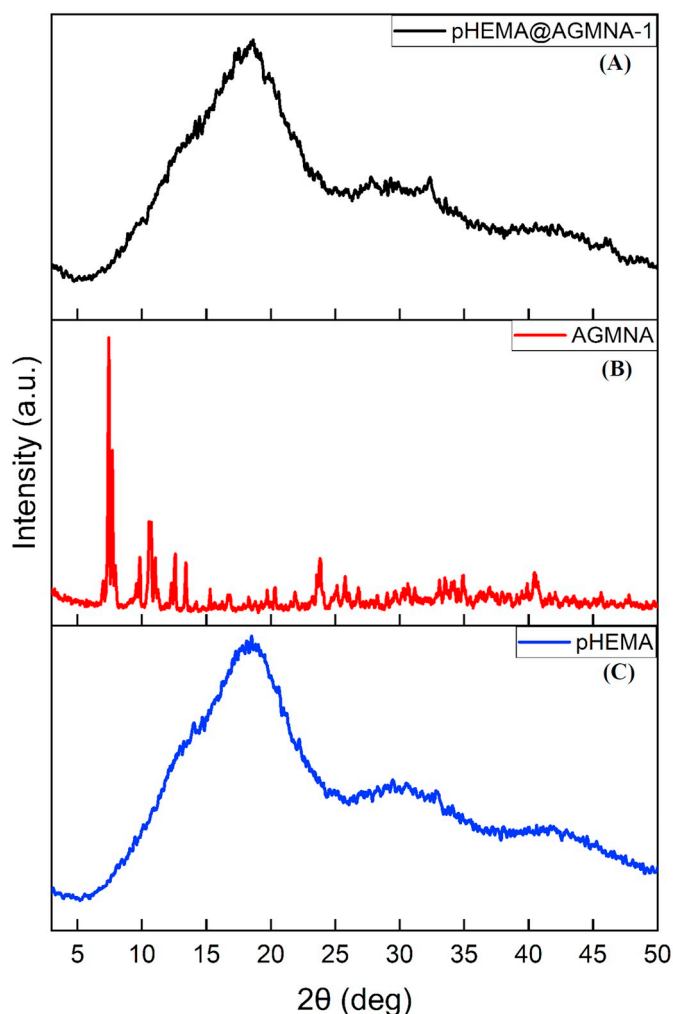


Fig. 3. X-ray diffraction analysis of pHEMA@AGMNA-1 (A), AGMNA (B) and pHEMA (C), respectively.

the disc is developed if the compound stops the bacterial growth or it kills them [20]. This is the so-called inhibition zone (IZ) [20]. Thus, discs of pHEMA or pHEMA@AGMNA-1 with diameter 10 mm, were placed to petri agar dishes and their inhibition zones (IZ) against *P. aeruginosa*, *S. epidermidis* and *S. aureus* were determined. The inhibition zones of pHEMA@AGMNA-1 against *P. aeruginosa*, *S. epidermidis* and *S. aureus* were 14.0 ± 1.1 mm, 11.3 ± 1.3 mm and 11.8 ± 1.8 mm, while no inhibition zones were developed when pHEMA was used (Fig. 9). Therefore, negligible IZs were developed when microbes were incubated with either pHEMA@AGMNA-1 or pHEMA. However, when soaked paper discs, of diameter of 10 mm with a solution of AGMNA (1 mM), were used, broad inhibition zones of 21.8 ± 0.8 mm [20], 23.5 ± 0.9 mm and 21.1 ± 0.4 mm against *P. aeruginosa*, *S. epidermidis* and *S. aureus* respectively were developed [20]. Since the agar diffusion test showed that pHEMA@AGMNA-1 discs develop insignificant IZs against *P. aeruginosa*, *S. epidermidis* and *S. aureus* (14.0, 11.3, 11.8 mm respectively), a minor releasing of the discs ingredient, could be concluded.

Although, a strong antimicrobial activity was exhibited, when pHEMA@AGMNA-1 discs are in contact with the microbes (inhibition rates of 99.6%, 98.5% and 92.3% against *P. aeruginosa*, *S. epidermidis* and *S. aureus*, respectively, see above), however, upon pHEMA@AGMNA-1 discs removal the remain solution still develop colonies on the agarose (Fig. 8).

2.10. *In vitro* toxicity of pHEMA@AGMNA-1 against normal human corneal epithelial cells (HCEC cells)

The *in vitro* toxic effect of pHEMA@AGMNA-1 discs against normal human corneal epithelial cells (HCEC cells) was evaluated for 24 h by SRB assay. The control cells were defined as the incubated cells with the pure pHEMA. The cell viability of HCEC upon their incubation with the discs of pHEMA@AGMNA-1 for 24 h was determined by $94.3 \pm 0.9\%$, indicating the non-toxicity of the discs towards HCEC cells.

2.11. *In vivo* toxicity evaluation, by brine shrimp *Artemia salina*

The materials, including pHEMA from which hydrogel lenses are made have received approval from U.S. Food and Drug Administration (F.D.A.) long time ago [27]. Moreover, AGMNA shows no *in vitro* and *in vivo* toxicity or genotoxicity against HCEC [20]. Therefore, the *in vitro* toxicity of the pHEMA@AGMNA-1 in comparison with the corresponding one of pHEMA is reported here using brine shrimp *Artemia salina* assay. Although, brine shrimp assay is not the appropriate *in vivo* cytotoxicity test for contact lens, however this model was used, due to ellipse of an animal model, in our laboratory. The brine shrimp *Artemia salina* lethality test has been reported to be a convenient preliminary toxicity test, useful in predicting biological activities such as cytotoxic, phototoxic and pesticidal activities [28]. Cytotoxicity as well as a wide range of pharmacological activities of bioactive compounds can be evaluated with brine shrimp lethality bioassay [29]. Thus, the brine shrimp *Artemia salina* test is widely used for toxicity tests due to its widespread distribution, short life cycle, non-selective grazing, and sensitivity to toxic substances [30,31]. Moreover, toxicity to brine shrimp coincides with toxicity to mammalian cells in many cases. However, there is no correlation in the degree of toxicity between the two systems [32].

The individuals of *Artemia salina* larvae, which survive in solutions with or without pHEMA@AGMNA-1 or pHEMA discs after 2, 4, 6, 8 and 24 h are summarized in Table 2. The lethality was noted in terms of deaths of larvae. No mortality rate of brine shrimp larvae was found upon incubation of pHEMA@AGMNA-1 and pHEMA for 2, 4, 6, 8 and 24 h, indicating their non-toxic behavior. Moreover, *Allium cepa* test reveals that AGMNA possesses no *in vivo* mutagenic or genotoxic effect [20].

The IC_{50} value after incubation of normal Human Corneal Epithelial cells (HCEC) with AGMNA is higher than $120 \mu\text{M}$ suggesting no *in vitro* toxicity. Moreover, whereas, the micronucleus frequency observed in the HCEC cells, without treatment is $2.20 \pm 0.19\%$, those treated with AGMNA at the concentration of $120 \mu\text{M}$ is $2.55 \pm 0.13\%$ [20]. This confirms the non *in vitro* genotoxic effects of AGMNA [20].

3. Conclusions

AGMNA, a silver cluster was successfully incorporated within pHEMA (lens polymer) during the polymerization process. This was verified by means of plethora of analytical methods including XRF, XRPD, SEM-EDX, TG-DTA/DSC, ATR-FTIR and Ultrasonic Imaging. The pHEMA@AGMNA-1 exhibited superior antimicrobial properties as compared to the pHEMA against *P. aeruginosa*, *S. epidermidis* and *S. aureus*. Finally pHEMA@AGMNA-1 not only resists against the microbial strains which are responsible for MK but it eliminates their colonies upon their contact with it. The absence of *in vitro* and *in vivo* toxicity and genotoxicity of AGMNA against HCEC cells and *Allium cepa* suggests that it would be a reasonable candidate for preparation of non-infectious contact lens.

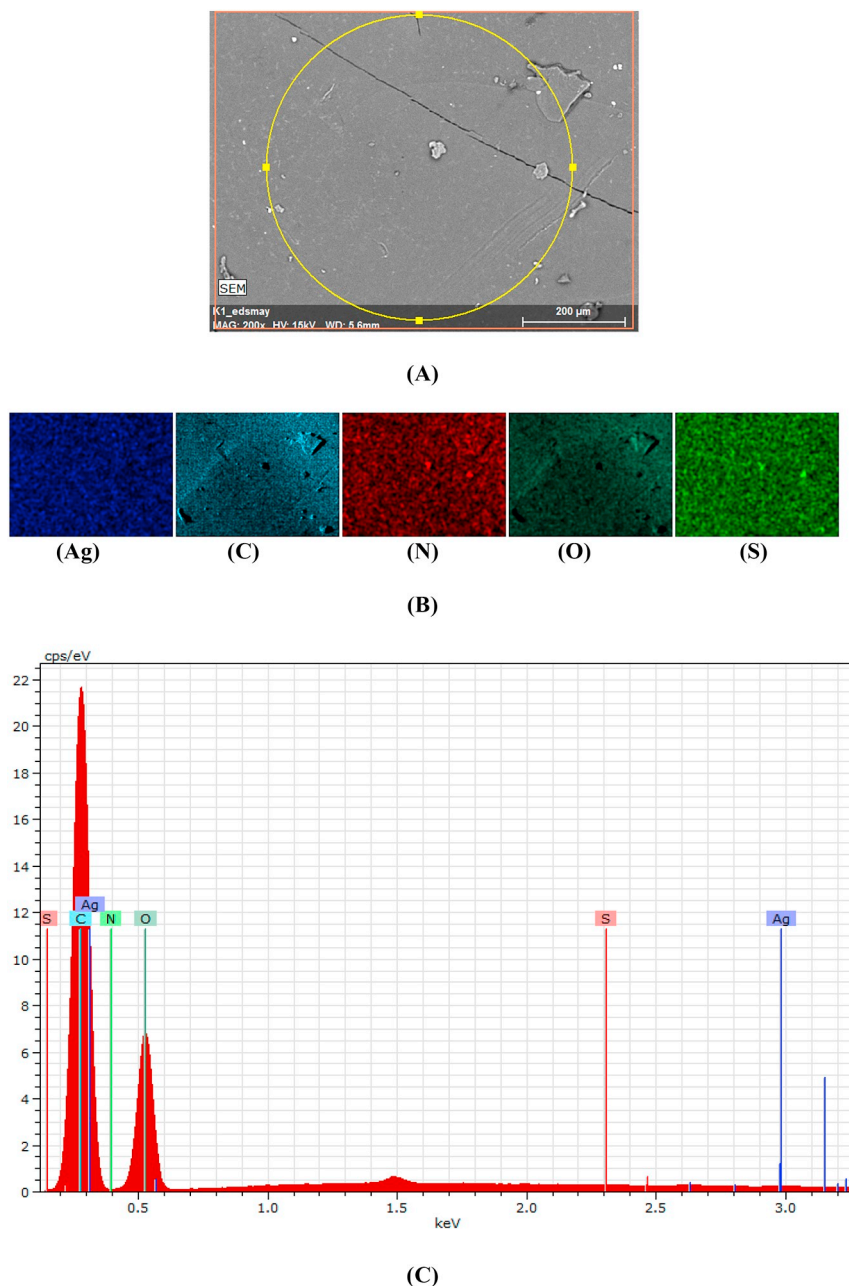


Fig. 4. (A) SEM image accompanied by EDX qualitative analysis. The cycle marks the location of EDX (B) EDX chemical maps (C) EDX analysis of pHEMA@AGMNA-1 surface.

4. Experimental

4.1. Materials and instruments

All used solvents were of reagent grade. 3-ethylene-amine (Et_3N , MERCK), 2-thio-nicotinic acid (H_2MNA , Aldrich), dimethylsulfoxide (DMSO, Riedel-de Haën) and silver nitrate (AgNO_3 , Degussa) were used for AGMNA synthesis without any further purification. Potassium bromide (KBr) for IR and ATR measurements was used in the form of fine-grained powder. For the lens preparation, 2-hydroxyethyl-methacrylate (pHEMA), ethylene-glycole-dimethacrylate (EGDMA, MERCK), diphenyl (2,4,6-trimethylbenzoyl) phosphine oxide (TPO 97%, Sigma Aldrich) as well as sodium chloride (NaCl, MERCK) and hydrochloric acid (HCl 37%, MERCK) were used. Tryptone tryptophan medium, beef extract powder, peptone bacteriological, soy peptone were purchased from Biolife. Agar and yeast extract were purchased from Fluka

Analytical. Sodium chloride, d(+)-glucose, di-potassium hydrogen phosphate trihydrate were purchased from Merck. Dimethyl sulfoxide was purchased from Riedel-de Haën. For the toxicity controls, brine shrimp eggs (*Artemia salina*) were purchased from Ocean Nutrition. Melting points were measured in open tubes with a Stuart Scientific apparatus and are uncorrected.

4.2. Synthesis and crystallization of AGMNA

AGMNA was synthesized as described in a previous work [20]. A clear solution of 0.5 mmol AgNO_3 (0.085 g) and 0.5 mmol of H_2MNA (0.075 g) were stirred in DMSO (5 mL) for 30 min. The solution was treated with 500 μL of tri-ethylamine (Et_3N) under continuous stirring for 180 min. Crystals of pure AGMNA were grown from slow evaporation of the solution after 2 days.

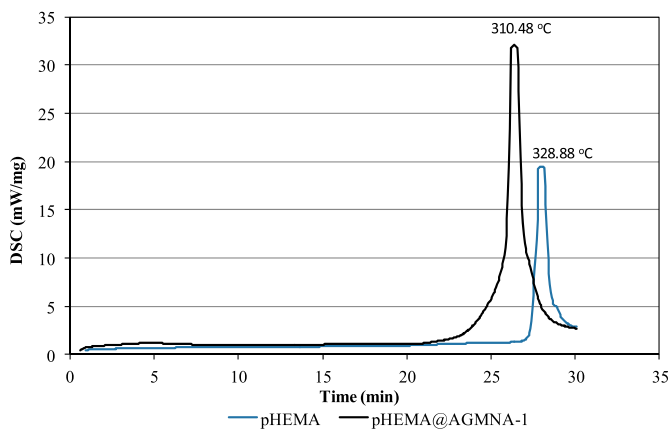


Fig. 5. DSC thermograms of pHEMA vs pHEMA@AGMNA-1.

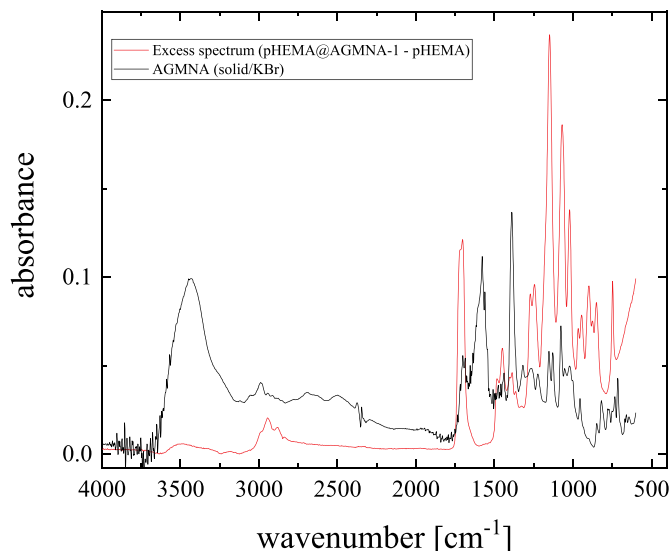


Fig. 6. The ATR-FT-IR spectrum of pHEMA@AGMNA-1 free from the vibration bands of pHEMA in comparison to the corresponding spectrum of AGMNA/KBr.

AGMNA: White-yellow crystal, melting point: 218–220 °C; IR (cm^{-1}), (KBr): 3405br, 2977w, 2676w, 2486w, 1669w, 1570 vs, 1471w, 1433w, 1385 vs, 1313s, 1248w, 1209w, 1149s, 1125w, 1076s, 1032w, 1015w, 945w, 802w, 751w, 713s, 715s, 659w, 639w, 574w, 470s.

4.3. Synthesis of pHEMA@AGMNA-1

Hydrogel of pHEMA with incorporated AGMNA is obtained as follows: 2.7 mL of HEMA were mixed with 2 mL of double distilled water (ddw), which contains AGMNA (1 mM) and 10 μL of EGDMA. The solution was then degassed by bubbling with nitrogen for 15 min. TPO initiator (6 mg) was added to the solution and mixed for 5 min at 800 rpm. The solution was poured into the mold and was then placed under a UV mercury lamp ($\lambda_{\text{max}} = 280 \text{ nm}$), 15 watt, where photopolymerization was occurred, for 40 min. Un-reacted monomers were removed, by immersed the gel in boiling water for 15 min. Discs with 10 mm diameter were cut, and they washed by immersion in water, NaCl 0.9%, HCl 0.1 M, and again in water. The discs were then dried at 40 °C until no weight change would occur. The yield of dry pHEMA and pHEMA@AGMNA is: 1.669 and 1.683 g respectively. For the antimicrobial activity tests, the hydrogel discs were stored in sterilized sodium chloride 0.9% w/w.

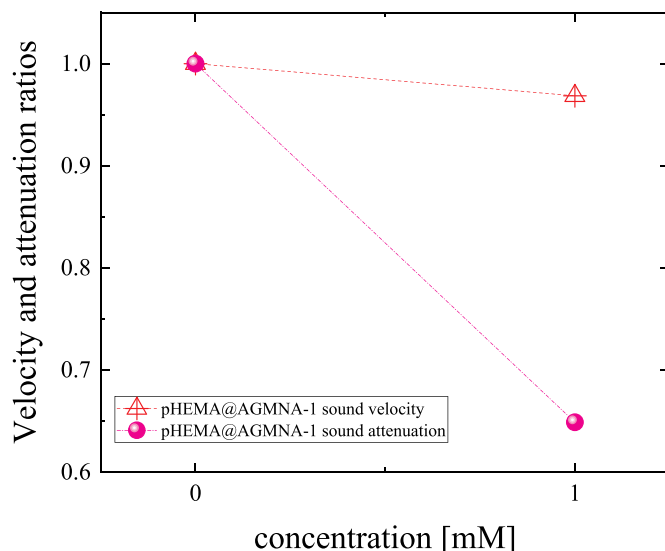


Fig. 7. Normalized velocity and attenuation ratios of pHEMA@AGMNA-1 with reference to unloaded pHEMA.

4.4. Refractive indices

The values of refractive indices of the lenses were measured with an Abbe refractometer (NAR-1T, Atago Co., Ltd., Tokyo) at 24 °C.

4.5. X-ray fluorescence spectroscopy

XRF measurement was carried out using an Am-241 radioisotopic source (exciting radiation 59.5 keV). For the detection of X-ray fluorescence a Si (Li) detector was used. The measuring time was chosen so as to collect ~ 2000 data on the weaker K α peak.

4.6. X-ray powder diffraction (XRPD)

The study of the samples by using the X-ray powder diffraction was accomplished by a diffraction-meter D8 AdvanceBruker, department of Physics, University of Ioannina. Radiation CuK α (40 kV, 40 mA, $\lambda_{\text{K}\alpha}$) and the monochromator system of diffracted beam were used. The X-ray powder diffraction patterns were measured in the area of 2θ angles between 2° and 80° using a rotation step 0.02° and time of 2 s per step. All samples measured with the above diffraction-meter were in fine-grained powder form.

4.7. Scanning Electron Microscopy (SEM), Energy-dispersive X-ray spectroscopy (EDX)

A Bruker EDAX equipment with XFlash detector coupled with Vega Tescan LMH II SEM was used for the elemental analysis of the synthesized sample.

4.8. Thermogravimetric Differential Thermal Analysis (TG-DTA), Differential Scanning Calorimetry (DTG/DSC)

For the DTA/TG measurements, a DTG/TG NETZSCH STA 449C was used. For the measurements, 10.9 mg of the sample were used, which were placed inside a platinum capsule on one side of the thermal-scale while on the other side α -alumina was used as reference sample. The speed of temperature increase was 10 °C/min at a temperature range of 25–500 °C and the measurements took place in the air. All the measured samples were in fine-grained powder form.

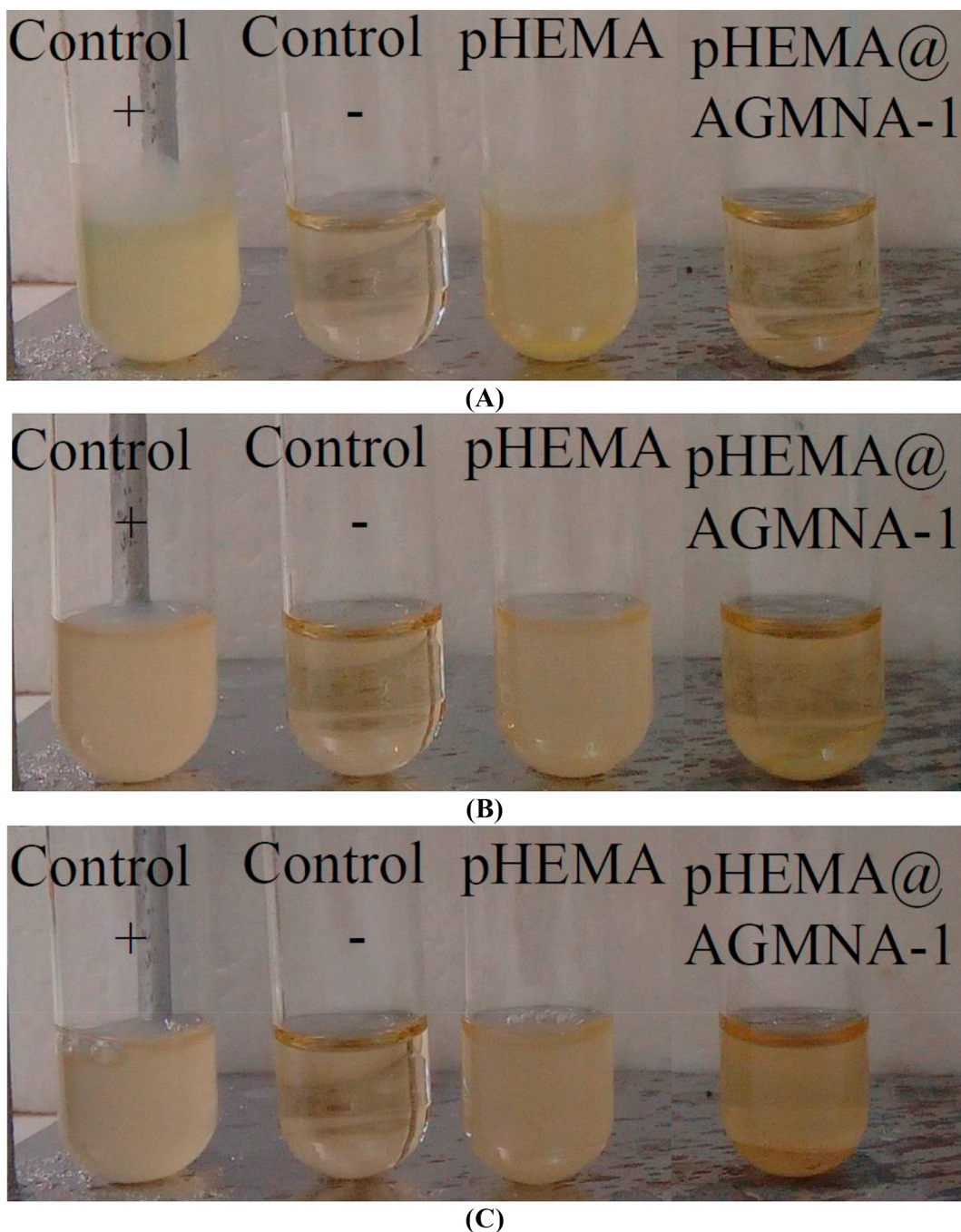


Fig. 8. Bacteria viability of pHEMA, and pHEMA@AGMNA-1 against *P. aeruginosa* (A), *S. epidermidis* (B) and *S. aureus* (C).

4.9. Attenuated total reflection spectroscopy (FT-IR-ATR)

The Fourier-transform infrared (FTIR) spectra were measured at room temperature using an Alpha spectrometer (Bruker) in transmittance mode using a DTGS detector. The spectral resolution for all measurements was set at 2 cm^{-1} . The spectra represent the average of 32 scans. Attenuated total reflectance (ATR) mid-infrared spectra were measured at room temperature utilizing the single reflection ZnSe crystal of the Horizontal ATR accessory attached to the sample compartment of the a Bruker Alpha FTIR spectrometer bearing the same DTGS detector. The penetration depth is up to $5\ \mu\text{m}$. After each measurement, the surface of the ZnSe crystal was cleaned with spectroscopic grade isopropanol. A background spectrum was recorded prior to any FTIR and ATR measurement using the atmospheric vapor

correction. Furthermore, all spectra were subjected to an internal standardization procedure allowing quantitative estimations.

4.10. Ultrasonic Imaging

In this work the changes in the ultrasonic velocity and attenuation have been used to monitor the incorporation of matrix by means of pulse-echo technique.

An X-cut wide-band transducer (Olympus NDT) with a fundamental frequency of 10 MHz was used to send and receive the longitudinal ultrasonic wave travelling through the sample at ambient conditions. A pulse generator (TTi, Model: TGR 1040) was utilized to excite the ultrasound transducer. The steady back wall echo train was monitored in a digital oscilloscope (TEKTRONIX, Model: TBS1152B, 150 MHz).

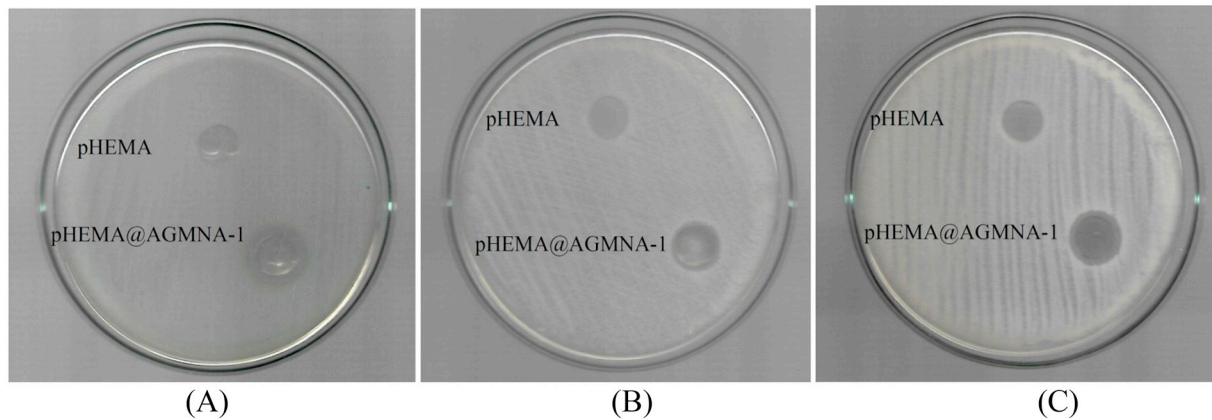


Fig. 9. Inhibition zones of pHEMA and pHEMA@AGMNA-1 against *P. aeruginosa* (A), *S. epidermidis* (B) and *S. aureus* (C).

Table 2

Number of *Artemia salina* larvae, which survive in solutions with or without pHEMA or pHEMA@AGMNA-1 discs after time interval of 2, 4, 6, 8 and 24 h.

		<i>Artemia salina</i> larvae					
		h					
		0	2	4	6	8	24
Control	Alive	9	9	9	9	9	9
	Non-alive	0	0	0	0	0	0
	Sum	9	9	9	9	9	9
pHEMA	Alive	7	7	7	7	7	7
	Non-alive	0	0	0	0	0	0
	Sum	7	7	7	7	7	7
pHEMA@AGMNA-1	Alive	6	6	6	6	6	6
	Non-alive	0	0	0	0	0	0
	Sum	6	6	6	6	6	6

The longitudinal velocity is calculated from the sample thickness d and the time separating two consecutive echoes in the back wall echo train with an accuracy of ± 5 m/s. The time between multiple reflections is estimated directly from the oscilloscope.

The attenuation coefficient α is defined from the exponential decrease of the sound pressure of the plane wave with respect to the travel distance when passing through the sample of thickness d . The amplitude of the attenuation coefficient is estimated with an accuracy of $\pm 2\%$ as:

$$\alpha(f) = \frac{-20}{2(m-n)d} \log\left(\frac{I_m}{I_n}\right)$$

where I_m and I_n are the amplitudes of the m -th and n -th pulse echoes, respectively. The acoustic attenuation is frequency-dependent and is attributed to the reflection, scattering and absorption of the acoustic waves in the medium.

4.11. Biological tests

4.11.1. Bacterial strains

The bacterial strains of *P. aeruginosa* (PAO1), *S. aureus* (ATCC® 25923™), and *S. epidermidis* (ATCC® 14990™), were adopted in the experiments. The bacterial strain *P. aeruginosa* PAO1, was kindly offered from Prof. A. Koukou (Laboratory of Biochemistry, University of Ioannina-Greece). The biological experiments were performed in triplicates. The values were evaluated by the statistical analysis software package included in the MS Office excel.

4.11.2. Effects of pHEMA and pHEMA@AGMNA-1 on the growth of microbial strains

The procedure was performed as previously reported [8,19,20]. Briefly, the bacterial strains were streaked onto in trypticase soy agar.

The plates were incubated for 18–24 h at 37 °C. Three to five isolated colonies are selected of the same morphological appearance from the fresh agar plate using a sterile loop and transfer into a tube containing 2 mL of sterile saline solution. The optical density at 620 nm is adjusted to 0.1 which corresponds in to 10^8 cfu/mL [8,19,20]. In order to evaluate the viability of microbes, pHEMA@AGMNA-1 and pHEMA discs were placed in tests tubes which contain $5 \cdot 10^5$ cfu/mL of *P. aeruginosa*, *S. epidermidis* and *S. aureus* microbes [8,19,20]. The optical densities of the supernatant solutions were then measured to give the % viability of microbes [8,19,20].

4.11.3. Removal of biofilm, caused by pHEMA@AGMNA-1 using crystal violet assay

Bacteria with a density of $1.3 \cdot 10^6$ cfu/mL were inoculated into LB medium for *P. aeruginosa* or tryptic soy broth for *S. aureus* (total volume = 1500 μ L) and cultured for 24 h at 37 °C. Afterwards, the content of each tube was carefully removed, the tubes were washed with 1 mL 0.9% saline dilution and 2 mL of broth were added. Negative control contained broth only. After that, the bacteria were incubated with pHEMA or pHEMA@AGMNA-1 for 20 h, at 37 °C. The content of each tube was aspirated and was washed three times with 1 mL methanol and 2 mL 0.9% saline and left to dry. Then, the tubes were stained for 15 min with crystal violet solution (0.1% w/v). Excess stain was rinsed off with 1 mL methanol and 2 mL 0.9% saline solution and after 3 mL 0.9% saline solution. The tubes are left to dry for 24 h and the bounded crystal violet was released by adding 30% glacial acetic acid. The optical density of the solution yielded is then measured at 550 nm, to give the biofilm biomass.

4.11.4. Determination of the inhibition zone (IZ)

The procedure was performed as previously reported [8,19,20]. Agar plates were inoculated with a standardized inoculum (10^8 cfu/mL) of the microorganisms. Discs of pHEMA or pHEMA@AGMNA-1 with 10 mm diameter were placed on the agar surface and the Petri plates were incubated for 20 h.

4.11.5. Sulforhodamine B assay

Initially, the HCEC cells were seeded in 24-well plate in a density of $7.5 \cdot 10^4$ cells and after 24 h of cell incubation, the discs of pHEMA and pHEMA@AGMNA-1 were added in the wells. After of 24 h incubation of HCEC cells with the discs, the discs were removed and the culture medium was aspirated and the cells were fixed with 300 μ L of 10% cold trichloroacetic acid (TCA). The plate was left for 30 min at 4 °C, washed five times with deionized water, and left to dry at room temperature for at least 24 h. Subsequently, 300 μ L of 0.4% (w/v) sulforhodamine B (Sigma) in 1% acetic acid solution was added to each well and left at room temperature for 20 min. SRB was removed, and the plate was washed five times with 1% acetic acid before air drying. Bound SRB was

solubilised with 1 mL of 10 mM un-buffered Tris-base solution. Absorbance was read in a 24-well plate reader at 540 nm [8].

4.11.6. Evaluation of toxicity with brine shrimp assay

Brine shrimp assay was performed by a method previously described [33]. 1 g cysts were initially hydrated in freshwater for 1 h in a separating funnel or cone shaped container. Seawater was prepared by dissolving 17 g of sea salt in 500 mL of distilled water [33,34]. The cone was facilitated with good aeration for 48 h at room temperature and under continuous illumination. After hatching, nauplii released from the egg shells were collected at the bright side of the cone (near the light source) by using micropipette. The larvae were isolated from the eggs by aliquoting them in small beaker containing NaCl 0.9% [35]. An aliquot (0.1 mL) containing about 6 to 10 nauplii was introduced to each well of 24-well plate and one disc of pHEMA or pHEMA@AGMNA-1 were added in each well. The final volume of each well is 1 mL with NaCl 0.9%. The brine shrimps were observed at the interval time of 2, 4, 6, 8 and 24 h, using a stereoscope. Larvae are considered dead if they do not exhibit any internal or external movement in 10 s of observation. Each experiment was repeated three times.

CRedit authorship contribution statement

A.K. Rossos: Investigation. **C.N. Banti:** Investigation, Methodology, Writing - original draft, Writing - review & editing. **A. Kalampounias:** Investigation. **C. Papachristodoulou:** Investigation. **K. Kordatos:** Investigation. **P. Zoumpoulakis:** Investigation. **T. Mavromoustakos:** Investigation. **N. Kourkoumelis:** Investigation. **S.K. Hadjikakou:** Conceptualization, Methodology, Supervision, Validation, Writing - original draft, Writing - review & editing.

Declaration of competing interest

The authors declare no any conflicts of interest.

Acknowledgements

This research has been co-financed by the European Union and Greek national funds through the Operational Program Competitiveness, Entrepreneurship and Innovation, under the call RESEARCH – CREATE – INNOVATE (project code:T1EDK-02990). Professor T. Vaimakis is acknowledged for the TG-DTA/DSC measurements. The COST Action CA15114 “Anti-Microbial Coating Innovations to prevent infectious diseases (AMICI)” is acknowledged for the stimulating discussions.

Appendix A. Supplementary data

Supplementary data to this article can be found online at <https://doi.org/10.1016/j.msec.2020.110770>.

References

- [1] M. Brothers, N.A. Stella, K.M. Hunt, E.G. Romanowski, X. Liu, J.K. Klarlund, R.M.Q. Shanks, Putting on the brakes: bacterial impediment of wound healing, *Sci. Rep.* 5 (2015) 14003.
- [2] K.F. Tabbara, H.F. El-Sheikh, B. Aabed, Extended wear contact lens related bacterial keratitis, *Br. J. Ophthalmol.* 85 (2001) 842.
- [3] A.B. Zimmerman, A.D. Nixon, E.F. Rueff, Contact lens associated microbial keratitis: practical considerations for the optometrist, *Clin. Optom.* 8 (2016) 1.
- [4] L. Szczołka-Flynn, R. Ahmadian, M. Diaz, A re-evaluation of the risk of microbial keratitis from overnight contact lens wear compared with other life risks, *Eye Contact Lens* 35 (2009) 69.
- [5] <https://www.cdc.gov/contactlenses/fast-facts.html>.
- [6] F. Stapleton, N. Carnt, Contact lens-related microbial keratitis: how have epidemiology and genetics helped us with pathogenesis and prophylaxis, *Eye* 26 (2012) 185.
- [7] A. Xiao, C. Dhand, L.-C. Ming, R.W. Beuerman, S. Ramakrishna, R. Lakshminarayana, Strategies to design antimicrobial contact lenses and contact lens cases, *J. Mater. Chem. B* 6 (2018) 2171.
- [8] I. Milionis, C.N. Banti, I. Sainis, C.P. Raptopoulou, V. Psycharis, N. Kourkoumelis, S.K. Hadjikakou, Silver ciprofloxacin (CIPAG): a successful combination of antibiotics in inorganic-organic hybrid for the development of novel formulations based on chemically modified commercially available antibiotics, *J. Biol. Inorg. Chem.* 23 (2018) 705.
- [9] S. Eckhardt, P.S. Brunetto, J. Gagnon, M. Priebe, B. Giese, K.M. Fromm, Nanobio silver: its interactions with peptides and bacteria, and its uses in medicine, *Chem. Rev.* 113 (2013) 4708.
- [10] C.-S.-A. Musgrave, F. Fang, Contact lens materials: a materials science perspective, *Materials* 12 (2019) 261.
- [11] O. Wichterle, D. Lim, Hydrophilic gels for biological use, *Nature* 185 (1960) 117.
- [12] M.I. Gonzalez-Sanchez, S. Perni, G. Tommasi, N. Glyn Morris, K. Hawkins, E. Lopez-Cabarcos, P. Prokopovich, Silver nanoparticle based antibacterial methacrylate hydrogels potential for bone graft applications, *Mater. Sci. Eng. C* 50 (2015) 332.
- [13] F.M. Helaly, S.M. El-Sawy, A.I. Hashem, A.A. Khattab, R.M. Mourad, Synthesis and characterization of nanosilver-silicone hydrogel composites for inhibition of bacteria growth, *Cont. Lens Anterior Eye* 40 (2017) 59.
- [14] R. Mourad, F. Helaly, O. Darwesh, S. El-Sawy, Antimicrobial and physicochemical natures of silver nanoparticles incorporated into silicone-hydrogel films, *Cont. Lens Anterior Eye* 42 (2019) 325.
- [15] M. Shayani Rad, B. Khameneh, Z. Sabeti, S. Ahmad Mohajeri, B. Sedigheh Fazly Bazzaz, Antibacterial activity of silver nanoparticle-loaded soft contact lens materials: the effect of monomer composition, *Curr. Eye Res.* 41 (2016) 1286.
- [16] L. Kyros, C.N. Banti, N. Kourkoumelis, M. Kubicki, I. Sainis, S.K. Hadjikakou, Synthesis, characterization, and binding properties towards CT-DNA and lipoxigenase of mixed-ligand silver(I) complexes with 2-mercaptothiazole and its derivatives and triphenylphosphine, *J. Biol. Inorg. Chem.* 19 (2014) 449.
- [17] I. Sainis, C.N. Banti, A.M. Owczarzak, L. Kyros, N. Kourkoumelis, M. Kubicki, S.K. Hadjikakou, New antibacterial, non-genotoxic materials, derived from the functionalization of the anti-thyroid drug methimazole with silver ions, *J. Inorg. Biochem.* 160 (2016) 114.
- [18] A. Papadimitriou, I. Ketikidis, M.K. Stathopoulou, C.N. Banti, C. Papachristodoulou, L. Zoumpoulakis, S. Agathopoulos, G.V. Vagenas, S.K. Hadjikakou, Innovative material containing the natural product curcumin, with enhanced antimicrobial properties for active packaging, *Mater. Sci. Eng. C* 84 (2018) 118.
- [19] M.-E.K. Stathopoulou, C.N. Banti, N. Kourkoumelis, A.G. Hatzidimitriou, A.G. Kalampounias, S.K. Hadjikakou, Silver complex of salicylic acid and its hydrogel-cream in wound healing chemotherapy, *J. Inorg. Biochem.* 181 (2018) 41.
- [20] M.P. Chrysouli, C.N. Banti, I. Milionis, D. Koumasi, C.P. Raptopoulou, V. Psycharis, I. Sainis, S.K. Hadjikakou, A water-soluble silver(I) formulation as an effective disinfectant of contactlenses cases, *Mater. Sci. Eng. C* 93 (2018) 902.
- [21] A.D. Cook, R.D. Sagers, W.G. Pitt, Bacterial adhesion to poly(HEMA)-based hydrogels, *J. Biomed. Mater. Res.* 27 (1993) 119.
- [22] A. Muñoz-Bonilla, D. López, M. Fernández-García, Providing antibacterial activity to poly(2-hydroxy ethyl methacrylate) by copolymerization with a methacrylic thiazolium derivative, *Int. J. Mol. Sci.* 19 (2018) 4120.
- [23] A.G. Kalampounias, S.N. Yannopoulos, W. Steffen, L.I. Kirillova, S.A. Kirillova, Short-time dynamics of glass-forming liquids: phenyl salicylate (salol) in bulk liquid, dilute solution, and confining geometries, *J. Chem. Phys.* 118 (2003) 8340.
- [24] P. Mpourazanis, G. Stogiannidis, S. Tsigoiias, G.N. Papatheodorou, A.G. Kalampounias, Ionic to covalent glass network transition: effects on elastic and vibrational properties according to ultrasonic echography and Raman spectroscopy, *J. Phys. Chem. Solids* 125 (2019) 43.
- [25] H. Ping, Determination of ultrasonic parameters based on attenuation and dispersion measurements, *Ultrason. Imaging* 20 (1998) 275.
- [26] A.M. El-Ganiny, G.H. Shaker, A.A. Aboelazm, H.A. El-Dash, Prevention of bacterial biofilm formation on soft contact lenses using natural compounds, *J. Ophthalmic. Inflamm. Infect.* 7 (2017) 11.
- [27] T. Grosvenor, Soft contact lenses: a look into the future, in: S.J. Cool, E.L. Smith (Eds.), *Frontiers in Visual Science, Springer Series in Optical Sciences*, 8 Springer, Berlin, Heidelberg, 1978.
- [28] S.M. Lee, B.S. Min, Y.H. Kho, Brine shrimp lethality of the compounds from *Phryma leptostachya* L. *Arch. Pharm. Res.* 25 (2002) 652.
- [29] S.B. Gajera, J.V. Mehta, M.N. Patel, Design of multifunctional iridium(III) compounds as a potential therapeutic agents from basic molecular scaffolds, *ChemistrySelect* 1 (2016) 3966.
- [30] R.A.F. Neves, T. Fernandes, L.N. dos Santos, S.M. Nascimento, Toxicity of benthic dinoflagellates on grazing, behavior and survival of the brine shrimp *Artemia salina*, *PLoS One* 12 (2017) e0175168.
- [31] M. Faimali, V. Giussani, V. Piazza, F. Garaventa, C. Corrà, V. Asnaghi, D. Privitera, L. Gallus, R. Cattaneo-Vietti, L. Mangialajo, M. Chiantore, Toxic effects of harmful benthic dinoflagellate *Ostreopsis ovata* on invertebrate and vertebrate marine organisms, *Mar. Environ. Res.* 76 (2012) 97.
- [32] M. de las M. Oliva, N. Gallucci, J.A. Zygadlo, M.S. Demo, Cytotoxic activity of Argentinean essential oils on *Artemia salina*, *Pharm. Biol.* 45 (2007) 259.
- [33] K. Rahman, S. Ullah Khan, S. Fahad, Z. Khan Shinwari, D. Khan, S. Kamal, I. Ullah, S. Ishfaq Anjum, S. Man, A. Jamil Khan, W. Ullah Khan, M. Hafeez Ullah Khan, M. Jan, M. Adnan, M. Noor, In vitro biological screening of a critically endangered medicinal plant, *Atropa acuminata* Royle Ex Lindl of north western Himalaya, *Sci. Rep.* 8 (2018) 11028.
- [34] V.V. Arun, N. Saharan, V. Ramasubramanian, A.M. Babitha Rani, K.R. Salin, R. Sontakke, H. Haridas, D.G. Pazhayamadom, Multi-response optimization of *Artemia* hatching process using split-split-plot design based response surface methodology, *Sci. Rep.* 7 (2017) 40394.
- [35] A. Rani Muhamad Syahmi, S. Vijayaratna, S. Sasidharan, L. Yoga Latha, Y. Ping Kwan, Y. Ling Lau, L. Ngit Shin, Y. Chen, Acute oral toxicity and brine shrimp lethality of *Elaeis guineensis* Jacq., (oil palm leaf) methanol extract, *Molecules* 15 (2010) 8111.